Accepted Manuscript

Design, synthesis, and biological evaluation of NAD(P)H: Quinone oxidoreductase (NQO1)-targeted oridonin prodrugs possessing indolequinone moiety for hypoxia-selective activation

Shengtao Xu, Hong Yao, Lingling Pei, Mei Hu, Dahong Li, Yangyi Qiu, Guangyu Wang, Liang Wu, Hequan Yao, Zheying Zhu, Jinyi Xu

PII: S0223-5234(17)30214-3

DOI: 10.1016/j.ejmech.2017.03.055

Reference: EJMECH 9315

To appear in: *European Journal of Medicinal Chemistry*

Received Date: 12 January 2017

Revised Date: 22 March 2017

Please cite this article as: S. Xu, H. Yao, L. Pei, M. Hu, D. Li, Y. Qiu, G. Wang, L. Wu, H. Yao, Z. Zhu, J. Xu, Design, synthesis, and biological evaluation of NAD(P)H: Quinone oxidoreductase (NQO1)-targeted oridonin prodrugs possessing indolequinone moiety for hypoxia-selective activation, *European Journal of Medicinal Chemistry* (2017), doi: 10.1016/j.ejmech.2017.03.055.

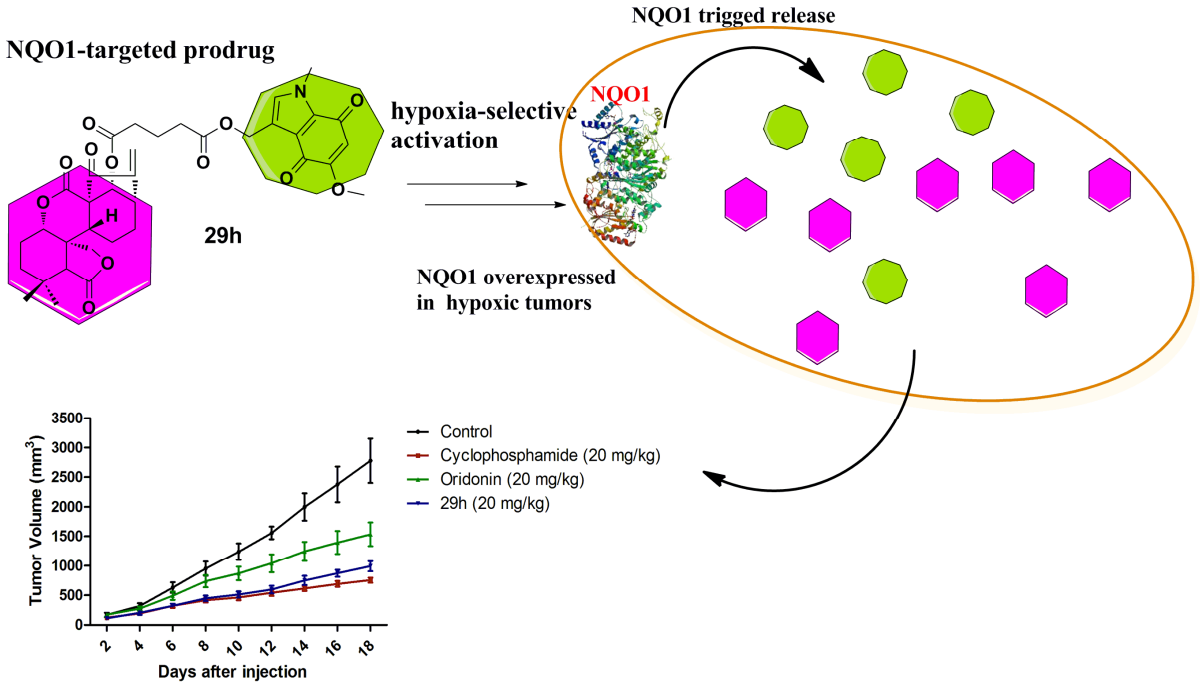

Design, synthesis, and biological evaluation of NAD(P)H: quinone oxidoreductase (NQO1)-targeted oridonin prodrugs possessing indolequinone moiety for hypoxia-selective activation

Shengtao Xu[a,1], Hong Yao[a,1], Lingling Pei[a], Mei Hu[a], Dahong Li[a,b], Yangyi Qiu[a], Guangyu Wang[a], Liang Wu[a,c,*], Hequan Yao[a], Zheying Zhu[d,*], Jinyi Xu[a,*]

[a]State Key Laboratory of Natural Medicines and Department of Medicinal Chemistry, China Pharmaceutical University, 24 Tong Jia Xiang, Nanjing 210009, P. R. China

[b]Key Laboratory of Structure-Based Drug Design & Discovery of Ministry of Education and School of Traditional Chinese Materia Medica, Shenyang Pharmaceutical University, 103 Wen Hua Road, Shenyang 110016, P. R. China

[c]Jiangsu Key Laboratory of Drug Screening, China Pharmaceutical University, 24 Tong Jia Xiang, Nanjing 210009, P. R. China

[d]Division of Molecular Therapeutics & Formulation, School of Pharmacy, The University of Nottingham, University Park Campus, Nottingham NG7 2RD, U.K.

***Correspondence should be addressed to:**

Biology: Z.Y. Zhu (Zheying.Zhu@nottingham.ac.uk); L. Wu (wul2004@hotmail.com)

Chemistry: J.Y. Xu (jinyixu @china.com)

Abstract: The enzyme NQO1 is a potential target for selective cancer therapy due to its overexpression in certain hypoxic tumors. A series of prodrugs possessing a variety of cytotoxic diterpenoids (oridonin and its analogues) as the leaving groups activated by NQO1 were synthesized by functionalization of 3-(hydroxymethyl)indolequinone, which is a good substrate of NQO1. The target compounds (**29a-m**) exhibited relatively higher antiproliferative activities against NQO1-rich human colon carcinoma cells (HT-29) and human lung carcinoma (A549) cells (IC_{50} = 0.263-2.904 μM), while NQO1-defficient lung adenosquamous carcinoma cells (H596) were less sensitive to these compounds, among which, compound **29h** exhibited the most potent

antiproliferative activity against both A549 and HT-29 cells, with IC_{50} values of 0.386 and 0.263 μM, respectively. Further HPLC and docking studies demonstrated that **29h** is a good substrate of NQO1. Moreover, the investigation of anticancer mechanism showed that the representative compound **29h** affected cell cycle and induced NQO1 dependent apoptosis through an oxidative stress triggered mitochondria-related pathway in A549 cells. Besides, the antitumor activity of **29h** was also verified in a liver cancer xenograft mouse model. Biological evaluation of these compounds concludes that there is a strong correlation between NQO1 enzyme and induction of cancer cell death. Thus, this suggests that some of the target compounds activated by NQO1 are novel prodrug candidates potential for selective anticancer therapy.

Keywords: NQO1; Oridonin; indolequinone; hypoxia-selective; antitumor

1. Introduction

Nonselective toxicity is a major factor that contributes to poor prognosis for cancer patients. One of the approaches to improve therapeutic effectiveness and decrease systemic side effects is design of targeted anticancer prodrugs for tumor site-specific activation [1]. A number of prodrug designs have been proposed to meet these requirements by taking advantages of low extracellular pH [2], elevated enzymes in tumor tissues [3], hypoxic environment inside the tumors [4], and so on [5]. Hypoxia is a common feature of most solid tumors, tissue hypoxia due to inadequate blood supply and rapid tumor growth will induce cancer cells resistant to radiotherapy and to many chemotherapeutic strategies [6]. However, tumor hypoxia also distinguishes tumor cells from normal cells, thus providing a unique strategy for selective cancer therapy [7]. Hypoxic cells prevalent in solid tumors could be selectively targeted by bio-reductive compounds whose activation is limited to hypoxic tumor regions thus minimizing the systemic side effects [8]. Hypoxia-activated prodrugs are activated by biotransformation following reductive metabolism by endogenous human cellular oxidoreductases [9].

Although a variety of oxidoreductases are known to be involved in prodrug

reduction, two-electron oxidoreductases NAD(P)H:quinone oxidoreductase (NQO1) is shown to be the most extensively researched [10]. NQO1 (E.C. 1.6.99.2, reduced nicotinamide adenine dinucleotide phosphate, also known as DT-diaphorase, DTD) is an obligate two electron quinone reductase. This flavoenzyme can utilize either NADH or NADPH to catalyze the reduction of various bio-reductive prodrugs [11]. NQO1 has received considerable attention in recent years for prodrug development, due to the fact that this enzyme is overexpressed in various types of tumors as compared with the paired normal tissue, making it an interesting target enzyme. Elevated levels of NQO1 in human tissues have been observed in primary tumors from lung (12- to 18-fold), liver (4- to 19-fold), colon (3- to 4-fold), and breast (3-fold) compared with normal tissue [12]. Therefore, NQO1 becomes an attractive target for enzyme-directed anticancer prodrugs designed for reductive activation.

Several classes of bio-reductive compounds that can undergo enzymatic reduction to active species have been developed [13-15]. Quinone is the structural moiety commonly associated with reductive activation which can be easily reduced by various reductive enzymes to hydroquinones[16]. Quinone is present in many bio-reductive compounds, such as mitomycin C (**1**), a clinically used antitumor antibiotic [17], and EO9 (**2**) that shows improved properties over mitomycin C [18], as well as other quinone-containing compounds (Figure 1) [19-20].

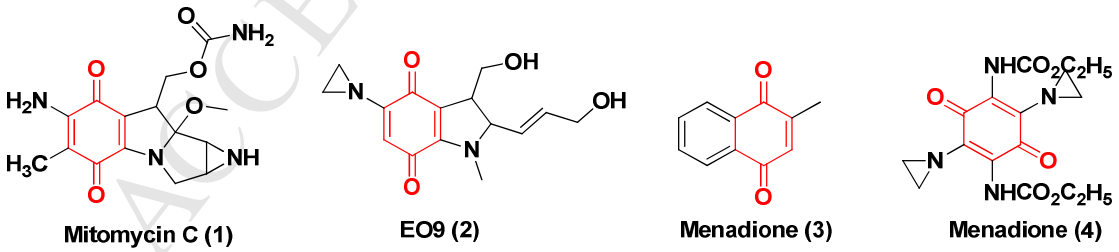

Figure 1. Chemical structures of antitumor quinones.

The indolequinone nucleus is the most common quinone which is a good substrate of NQO1 and can be activated through an obligate and non-reversible two-electron reduction. Recently, structure-activity relationship (SAR) analysis of the

indolequinone moiety and the molecular features relating to substrate specificity for human NQO1 has been examined [21-23]. Evidence indicates that substitution with a potential leaving group at the 3-position of the indolequinone moiety is a viable means for bio-reductive drug delivery [24]. Figure 2 shows a proposed mechanism for the release of drugs following reduction of the indolequinone prodrug **5**. When **5** is reduced by two electrons to dihydroxyindole **6** in the presence of NQO1, the electron-density at the indole nitrogen increases markedly, triggering expulsion of the leaving group **7**. This expulsion generates an alkenyliminium electrophile **8**, which is a potential electrophile capable of DNA-alkylation or other cellular-damaging events contributing to the cytotoxicity to tumor cells [25]. This reduction is often inhibited in the presence of oxygen, thus increasing the specificity for hypoxic solid tumors. Interestingly, if the leaving group **7** is a bioactive group, thus they may have secondary biological effects due to the eliminated molecule **7** [26-28]. As shown in Figure 2, there are two mechanisms through which indolequinone-based prodrugs can induce cytotoxicity. Firstly, the indolequinone structure itself can be converted to a reactive, cytotoxic species by reduction to a hydroquinone. Secondly, the indolequinone moiety can be used to form a prodrug that selectively releases other cytotoxic agents to hypoxic tissues. Thus, design and synthesis of NQO1-activated indolequinone prodrugs by functionalization at the (indol-3-yl)methyl position with a variety of cytotoxic leaving groups have become an interesting area to develop targeted anticancer prodrugs.

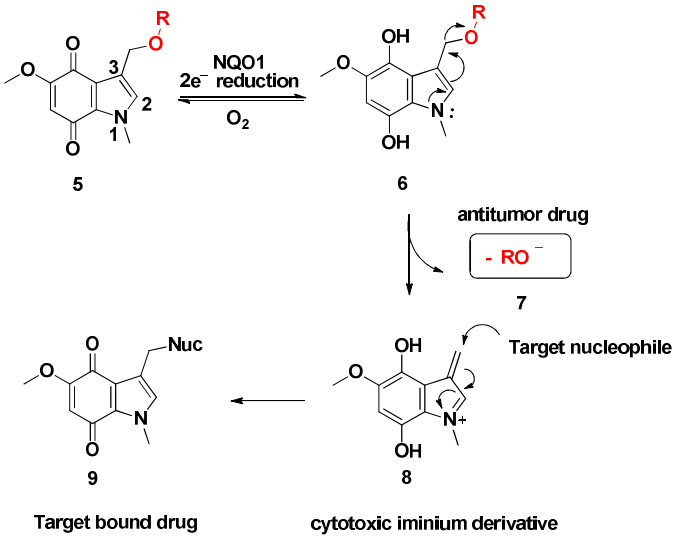

Figure 2. Schematic illustration for activation of NQO1-targeted prodrugs upon hypoxic irradiation.

Natural product oridonin (**10**), an *ent*-kaurene diterpenoid extracted from *Radosia Rubescens*, was firstly identified in 1967 as an antitumor agent [29-30]. Numerous researches have shown that oridonin has certain antitumor effects on human breast cancer, gallbladder cancer, leukemia, gastric cancer, human cervical carcinoma, hepatocellular carcinoma and other tumors [31]. In our previous studies, oridonin and its semi-synthesized analogues exhibited safe, unique, and extensive antitumor activities [32-34]. In the present study, a series of reductively triggered novel prodrugs were designed by substitution at the 3-position of the indolequinone nucleus with cytotoxic diterpenoids oridonin or its analogues. The active drug oridonin or its analogues were subsquently released under bio-reductive transformation by NQO1 which is overexpressed in tumor tissues. This design is expected to enhance drug specificity toward tumor cells and thus reduce side effects.

Herein, we report the design, synthesis and preliminary drug release study of NQO1-targeted oridonin prodrugs possessing indolequinone moiety for bio-reductively triggered drug release.

2. Results and discussion

2.1. Synthesis of NQO1-targeted oridonin prodrugs

The conversion of kaurene-type oridonin to 6,7-seco-kaurene-type compounds **12-13** was achieved by periodate. As shown in Scheme 1, treatment of **10** with sodium periodate in water gave **12** in 98% yield. Subsequent oxidation of **12** with Jones reagent at room temperature afforded lactone **13** in 90% yield. According to our previous report, treatment of **10** with 2,2-dimethoxypropane in the presence of TsOH in acetone provided ketal **14** in 95% yield [35]. Compound **14** upon reaction with Ac_2O/DMAP/TEA led to acetylated compound **15** in the yield of 92%. Then, deprotection of **15** with 10% HCl/THF gave the corresponding alcohol **16** in almost quantitative yield. Besides, the 1-hydroxy of compound **14** was selectively activated by MsCl, which was subsequently subjected to an elimination reaction in the presence of Li_2CO_3 and LiBr in DMF at 110 ^oC to provide 1-ene **19** in 85% yield. Removal of the acetonide group in **17** and **19** with 10 % HCl aqueous solution offered **18** and **20** in yield of 93 % and 95%, respectively.

Scheme 1. Synthesis of oridonin analogues **11**-**20**[a]

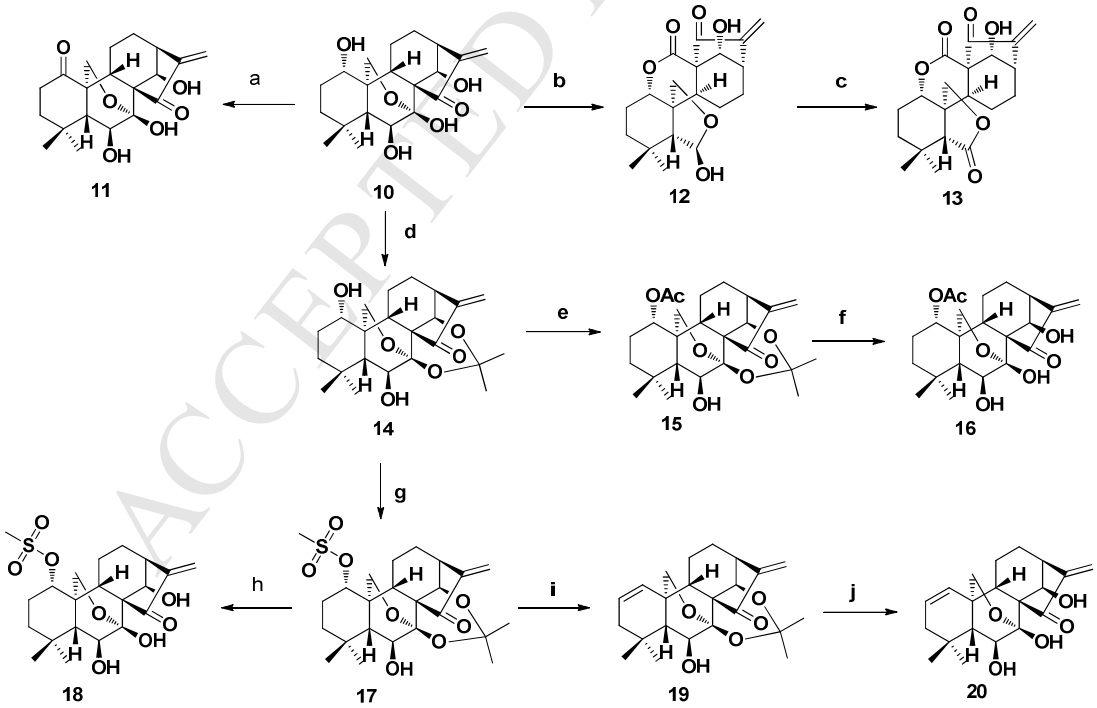

[a]Reagents and conditions: (a) Jones' reagent, acetone, 0 ^oC, 15 min, 94%; (b) $NaIO_4$, H_2O, rt, 24 h, 98%; (c) Jones' reagent, acetone, rt, 15 min, 90%; (d) 2,2-Dimethoxypropane, acetone, TsOH, 56 ^oC, 30 min, 95%; (e) Ac_2O, TEA, DMAP,

rt, 2 h, 92%; (f) 10% HCl, THF, rt, 30 min, 97%; (g) MsCl; TEA, 0 ^{o}C, 2 h, 88%; (h) 10% HCl, THF, rt, 20 min, 93%. (i) $LiCO_3$, LiBr, THF, 110 ^{o}C, 1 h, 85%; (j) 10% HCl, THF, rt, 30 min, 95%.

The synthesis of indolequinone skeleton was carried out as depicted in Scheme 2 starting from 5-methoxyindole (**21**) [36]. Briefly, formylation of **21** produced **22** in almost quantitative yield, methylation of **22** using methyl iodide in the presence of sodium hydride gave **23** in 95% yield. Nitration of **23** using conc. HNO_3 in acetic acid gave **24** in 73% yield. Reduction of the nitro group of **24** using Sn/HCl produced the amine **25** followed by oxidation using Fremy's salt to gave **26**, which was subsequently reduced using $NaBH_4$ to afford **27** in 70% yield. In order to install oridonin or its analogues at the 10-position of indolequinone, we converted the hydroxyl group of **27** into the carboxyl function to give compounds **28a-b** using succinic anhydride or glutaric anhydride. The target compounds **29a-n** were obtained by coupling **28a-b** with oridonin or its analogues through the condenstation reaction in the presence of EDCI and DMAP with 48-92% yields.

Scheme 2. Synthesis of NQO1-targeted prodrug candidates **29a-n**[a]

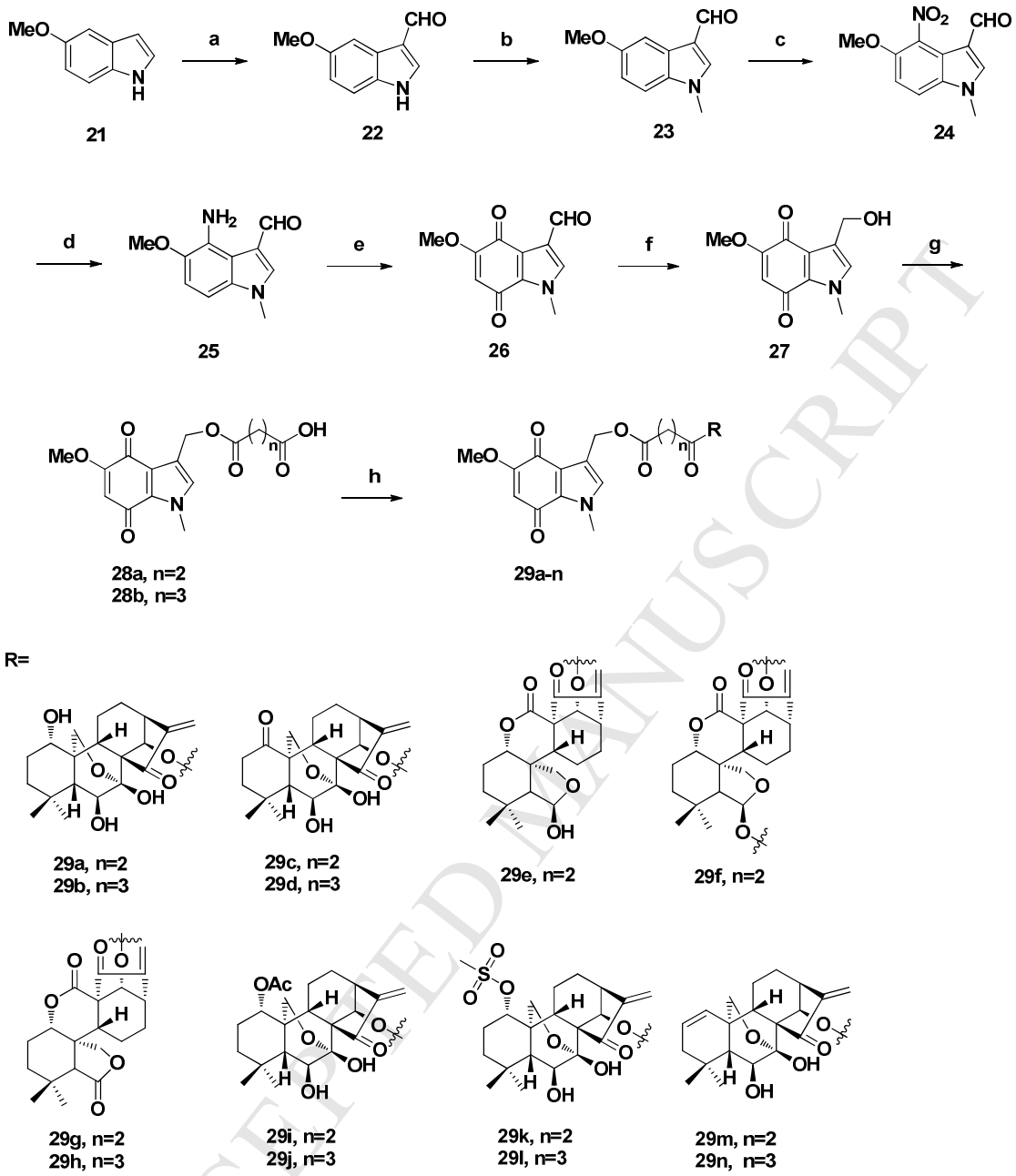

[a]Reagents and conditions: (a) $POCl_3$, DMF, 0 °C to rt, 2 h, 90%; (b) NaH, MeI, DMF, rt, 30 min, 95%; (c) HNO_3, AcOH, 10-15 °C, 73%; (d) Sn, HCl, MeOH, rt, 57%; (e) Fremy's salt, acetone, PBS pH=6.4, 3 h, 45%; (f) $NaBH_4$, MeOH, 10 min, 70%; (g) Anhydride, DMAP, DCM, rt, 12-24 h, 55%-80%; (h) EDCI, DMAP, rt, 0.5-24 h, 48-92%.

2.2. Effect of prodrugs on cancer cell growth

To assess the extent to which NQO1 contributes to the cytotoxicity of these

compounds, MTT assay was performed in three different tumor cell lines: human colon carcinoma cells (HT-29), human lung carcinoma cells (A549), and human lung adenosquamous carcinoma cells (H596). HT-29 and A549 cells have a high level of NQO1 activity, while H596 cells have a relative low level of NQO1 activity. Taxol was used as a positive control in this study. As shown in Table 1, most target compounds exhibited relatively higher anticancer activities against NQO1-rich A549 and HT-29 cell lines, with IC_{50} values ranging from 0.216 to 2.904 μM, whereas NQO1-defficient H596 cells were markedly less sensitive to these compounds. Selectivity ratios defined as IC_{50}(H596)/IC_{50}(A549) were generally > 1, except for compound **29a**, indicating that these compounds were more cytotoxic to the NQO1-rich cells due to activation by NQO1 enzyme. As compared to parent oridonin, NQO1 targeted prodrugs showed higher antiproliferative activities against all three cancer cell lines. Compounds **29h** and **29f** were at least 17 times more active than parent oridonin (**1**) against NQO1-rich cells. The difference was most notable in A549 cells, where **29h** was 59-fold more potent than oridonin. Among the tested compounds, compound **29h** exhibited the strongest antiproliferative activity against both A549 and HT-29 cells, with IC_{50} values of 0.386 and 0.263 μM, respectively, which deserves further investigations.

Table 1. IC_{50} values (μM) of final and reference compounds on inhibiting proliferation of human cancer and normal cells[a]

Compounds	IC_{50} (μM)[b]				Selectivity[c]
	HT-29 (NQO1+)	A549 (NQO1+)	H596 (NQO1-)	LO2	
Taxol	0.025	0.023	0.035	0.002	1.52
1	7.099	15.525	11.969	25.023	0.77
29a	1.112	2.904	1.699	7.907	0.59
29b	1.299	0.458	1.681	8.232	3.67
29c	0.755	1.077	1.650	5.539	1.53

29d	0.693	0.363	1.062	4.124	2.93
29e	1.119	2.596	3.747	4.893	1.44
29f	0.399	0.286	1.350	1.276	4.72
29g	0.344	0.524	0.890	1.096	1.70
29h	0.386	0.263	1.505	2.113	5.72
29i	1.054	0.689	1.863	7.722	2.70
29j	0.462	0.403	0.900	2.044	2.23
29k	1.715	2.067	2.631	6.087	1.27
29l	0.754	0.405	2.001	3.269	4.94
29m	0.527	0.729	0.782	1.590	1.07
29n	1.114	0.373	1.746	7.458	4.68

[a]MTT methods, cells were incubated with indicated compounds for 72h, the values are the means of three independent experiments; [b]HT-29, Human colon carcinoma cells (High NQO1 activity, NQO1+); A549, Human lung carcinoma cells (High NQO1 activity, NQO1+); H596, Human lung carcinoma cells (No NQO1 activity, NQO1-); LO2, Human normal liver cells; [c]Selectivity = IC_{50}(H596)/ IC_{50}(A549).

Consequently we measured the antiproliferative activities of three potent representative compounds **29f**, **29h**, **29n** in the presence of dicoumarol (DIC, 10 mM), an effective NQO1 inhibitor that blocks the catalytic efficiency of the enzyme by interacting with the NAD(P)H-binding site of the oxidized enzyme form. As shown in Figure 3A, the co-incubation with DIC led to lower sensitivity of A549 cells to compounds **29f**, **29h**, **29n**, and increasing IC_{50} values up to 7.5-, 4.5- and 5.9- fold, respectively, which implies that they might be partially influenced by their NQO1-catalyzed bio-reductive activation.

Furthermore, we found the synergic effect of compound **29h** in both A549 and H596 cells. As shown in Figure 3B, compound **29h** contains an oridonin analogue (compound **13**) and indolequinone (**27**) moieties, the IC_{50} values of **29h** for A549 (0.263 μM) and H596 cells (0.386 μM) were significantly less than that of the

equimolar combination of **13** and **27** (IC_{50} = 6.143 and 5.823 μM), respectively. These results suggest that the anti-tumor activity of **29h** may be attributed to the synergic effects of oridonin and indolequinone moieties as well as hypoxia-selective activation in cancer cells.

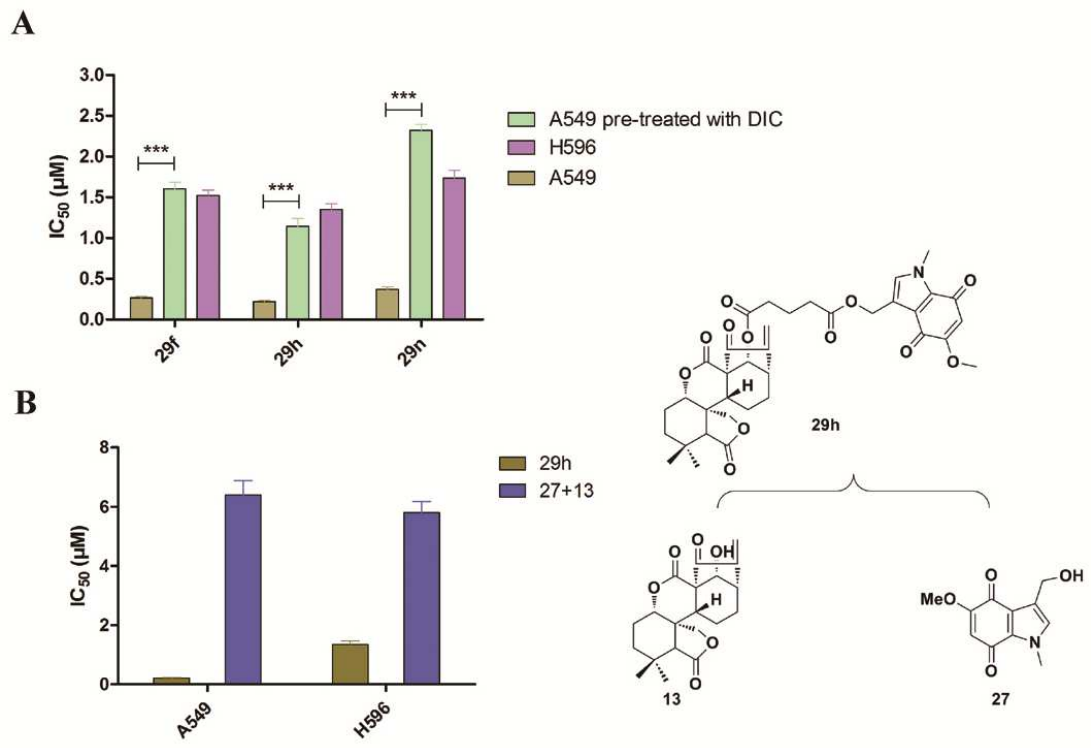

Figure 3. NQO1 contributes to the cytotoxicity of these newly designed indolequinone prodrugs. (A) Compounds induced cytotoxicity is NQO1 dependent. A549 cells were pretreated with 10 mM DIC for 30 min, then incubated with indicated compounds, DIC (dicoumarin), NQO1 inhibitor; (B) Comparison of anticancer activity of compound **29h** with that of equimolar mixture of **13** and **27**. MTT methods, cells were incubated with indicated compounds for 72h, (means ± SD, n=3).

*2.3. Compound **29h** is a good substrate of NQO1*

To assess the efficacy of these newly synthesized compounds as substrates for NQO1, HPLC analysis was used to monitor the decomposition of **29h** in the presence or absence of NQO1 in pH 7.4 buffer. Upon reduction with NQO1, the electron

density at the indole nitrogen increases drastically, triggering expulsion of the leaving group in a reverse-Michael-like process, releasing the drug at the 3-position of the indolequinone nuclear. As shown in Figure 4, within 40 min, a significant amount of **29h** was decomposed in the presence of NQO1, and in 12 h, nearly 70% of the compound was consumed. However, during the same time period, in the absence of NQO1, **29h** remained stable in pH 7.4 buffer suggesting NQO1 could mediate hypoxic induced, enzyme-directed bio-reductive drug delivery.

Moreover, docking study of representative compound **29h** was further performed to observe whether this prodrug is a good substrate of NQO1. The molecular operating environment (MOE) was used to analyse the binding mode of **29h** with NQO1, Figure 4B showed the possible docking conformation for **29h** with NQO1. It can be clearly seen that indolequinone moiety binds with the residues of the NQO1 active site and flavin adenine dinucleotide (FAD) which is required for NQO1 catalytic activity (Figure 4B). The leaving group **13** is left outside the substrate binding pocket, suggesting that the interaction of indolequinone with NQO1 active site is not affected by the introduction of oridonin or its analogues to indolequinone. This binding mode was consistent with the HPLC data indicating that **29h** is a good substrate for NQO1.

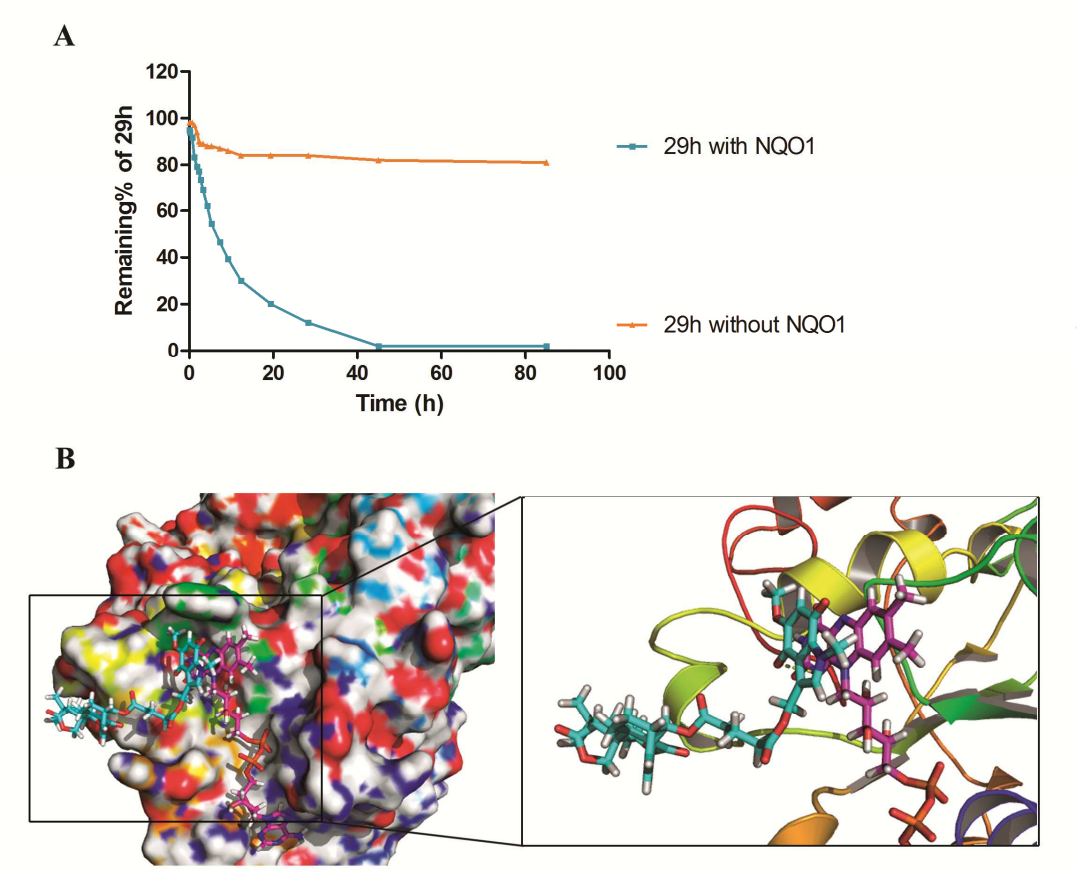

Figure 4. These newly synthesized prodrugs are good substrates of NQO1. (A) Decomposition profiles of **29h** in the presence and absence of NQO1 were determined by HPLC analysis. (B) Docked conformation of compound **29h** into active site of NQO1. The interaction mode was obtained through molecular docking (PDB id: 1h29) and depicted using PyMOL. FAD is expressed in magenta and **29h** is represented as stick model, nitrogen atoms are colored in blue, oxygen atoms are colored in red, and carbon atoms are colored in cyan. Hydrogen bonds are represented by dashed yellow lines along with their distances.

*2.4. Compound **29h** induces NQO1 dependent apoptotic cell death*

To further investigate the effect of **29h** on cell proliferation, Hoechst 33342 staining was used to assess **29h**-dependent changes in cell morphology. Both A549 and H596 cells treated with **29h** for 36 h displayed changed morphologies, over 12.6% of the H596 cells exhibited chromatin condensation upon 0.5 μM of **29h** treatment, indicating the induction of apoptosis (Figure 5A). However, chromatin condensation

was more obvious on A549 cells after treatment with 0.5 μM **29h**, approximately 30% cells exhibited changed morphologies. Furthermore TUNEL assays were performed to confirm that **29h** induced cell death is due to the induction of NQO1 dependent apoptosis. As shown in Figure 5B, **29h** induced a concentration dependent apoptosis in A549 cells and the TUNEL positive cells reached over 18.5% upon 0.5 μM of **29h** treatment, whereas the TUNEL positive cells detected from H596 cells upon **29h** treatment is of no difference from control treatment at this concentration. The results of TUNEL assays are in complete agreement with those from MTT based cytotoxicity studies, strongly suggesting that **29h** induces an NQO1 dependent apoptotic cell death in A549 cells.

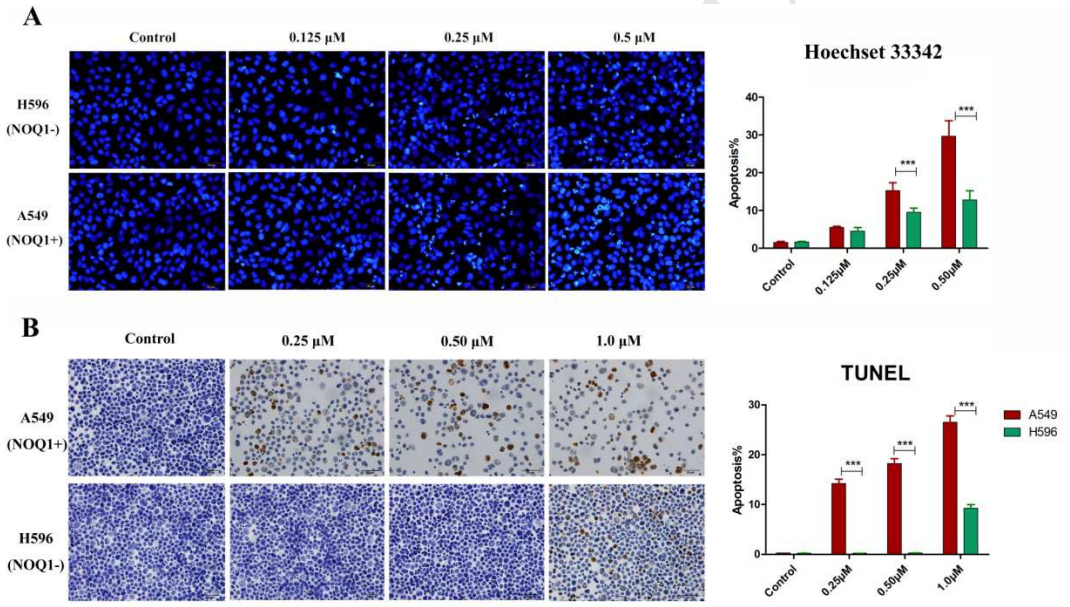

Figure 5. Evidence shows that compound **29h** induces apoptosis. (A) Cell morphological alterations and nuclear changes associated with A549 and H596 cells after **29h** treatment were assessed by staining with Hoechst 33342 and visualized by fluorescence microscopy. *** $p < 0.001$ compared between A549 and H596 groups. (B) TUNEL assay was used to identify apoptosis. Histograms display the percentage of apoptotic cells. Data were represented as mean ± SD of three independent experiments. *** $p < 0.001$ *vs* control group.

2.5. The role of ROS generation and mitochondrial membrane depolarization in 29h-induced cell apoptosis

Cellular reactive oxygen species (ROS) generation can significantly impact the effects of various anticancer agents on tumor cell apoptosis. We have found that **29h** was reduced by NQO1 to induce the apoptosis in A549 cells. In order to monitor intracellular ROS levels in the presence and absence of **29h**, DCF staining was applied to detect **29h** induced ROS formation. As shown in Figure 6A, DCF staining data displayed that **29h** induced excessive ROS formation in A549 cells but not in H596, and **29h** treated A549 cells had significantly higher levels of ROS than that in control cells. The above results indicated that ROS produced from NQO1 bio-activation is an important mediator on **29h** induced apoptotic cell death. ROS are considered to play an important role in apoptosis in various types of cells, and mitochondrial membrane depolarization is associated with mitochondrial production of ROS, therefore we measured the mitochondrial membrane potential (MMP) in both A549 and H596 cells with fluorescent probe JC-1. A549 cells were incubated with different concentrations (0, 0.25, 0.5, 1 μM) of **29h** for 48 h prior to staining with the JC-1, the number of cells with collapsed mitochondrial membrane potentials in different groups were determined by flow cytometry analysis, yielding 4.6%, 23.4%, 31.4%, and 46.3% apoptotic cells, respectively.

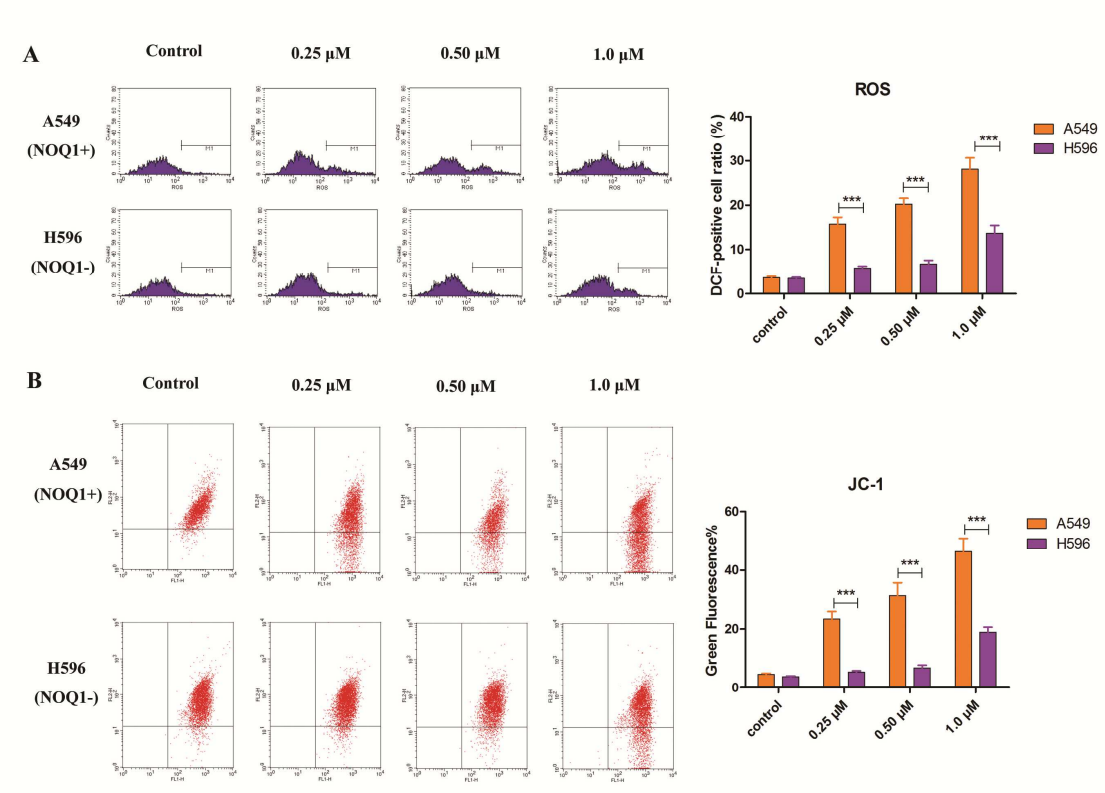

Figure 6. The depolarization of mitochondrial membrane potential and accumulation of ROS production induced by **29h** are required for cell apoptosis. (A) Effect of **29h** on ROS generation. The generation of ROS was measured by using the ROS-detecting fluorescent dye DCF-DA in combination with FACScan flow cytometry. The corresponding histograms of FACScan flow cytometry is shown; (B) Effect of compound **29h** on the mitochondrial membrane potentials of A549 cells. A549 cells were incubated with the indicated concentrations of compound **29h** for 48 h, cells were then collected and stained with JC-1, followed by flow cytometric analysis.

*2.6. Compound **29h** induces cell cycle arrest at G2/M phase*

Most of the antitumor agents inhibit cell proliferation through induction of cell cycle arrest [37]. To determine whether the suppression of the cell growth by **29h** was caused by a cell-cycle effect, DNA-based cell cycle analysis was performed using flow cytometry. As illustrated in Figure 7, compound **29h** influenced cell cycle progression at sub-micromolar concentrations and caused blockage of the cell cycle at

G2/M phase. Compared with the control cells treated with DMSO, when A549 cells were treated with increasing concentrations of **29h** (0.125, 0.25, 0.5 μM), the percentage of cells in the G2/M phase increased from 12.65 % to 26.57 %, and the percentages of cells in S and G1 phases decreased concomitantly. The above results suggested that these prodrugs may inhibit cancer cell proliferation through cell cycle arrest at G2/M phase.

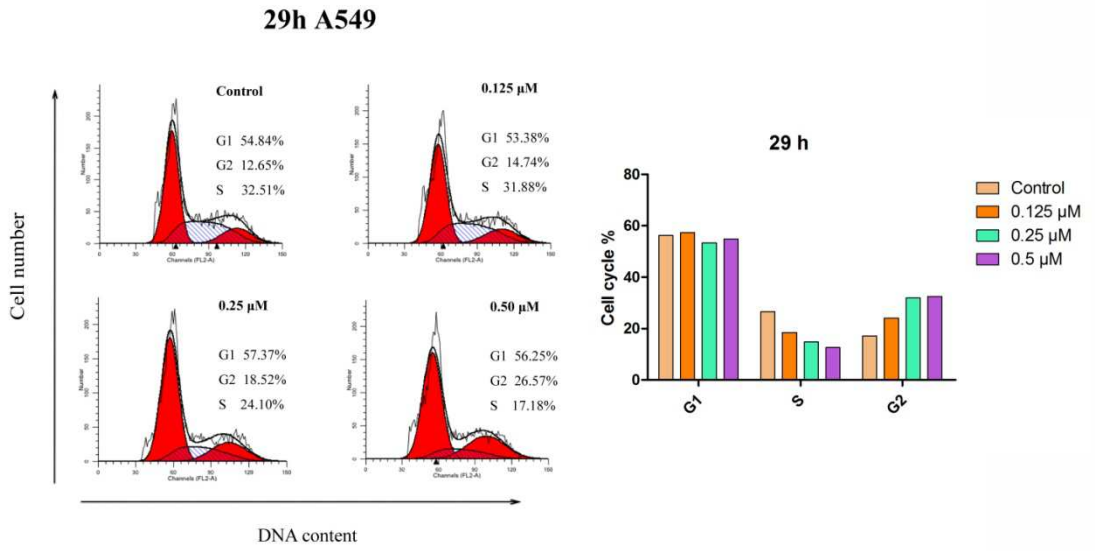

Figure 7. Compound **29h** induces G2/M phase arrest in the A549 cells. A549 cells were treated with DMSO and varying concentrations of **29h** (0.125, 0.25, 0.5 μM) for 48 h, cells were harvested and stained with PI, then analyzed by flow cytometry. The percentage of cells at different phases of cell cycle was determined by ModFit 4.1, histograms display the percentage of cell cycle distribution.

*2.7. Compound **29h** regulates apoptotic related proteins*

The intrinsic and extrinsic pathways that lead to the induction of apoptosis are known to activate a series of proteases known as caspases [38]. To explore the signalling mechanism of **29h**-induced apoptosis, we examined the expression of the apoptosis-related proteins including caspase-3, -8, -9, and cytochrome C. As shown in Figure 8A, A549 cells treated with **29h** had increased levels of the cleaved active forms of caspase-3, -8, -9, and cytochrome C in a dose-dependent manner, indicating

that **29h** activated the caspase cascade.

The Bcl-2 family has been identified as essential proteins in controlling the mitochondrial pathway. This family includes pro-apoptotic proteins (e.g., Bax, Bad) and anti-apoptotic proteins (e.g., Bcl-2, Bcl-xL), the balance between these two groups determines the fate of cells [39]. Bax can act on the mitochondria to induce the mitochondrial permeability transition, resulting in the release of some components, including cytochrome C. To confirm whether such a mechanism is involved in apoptosis induced by **29h**, the expression of Bax and Bcl-xl was examined by Western Blotting analysis. As shown in Figure 8B, the expression of Bax in A549 cells began to increase after the treatment of **29h** with increasing concentrations for 48 h, while the Bcl-xl expression markedly decreased at concentrations of 0.25 μM and above. While a similar trend was observed in H596 cells, however, such effect was minimal.

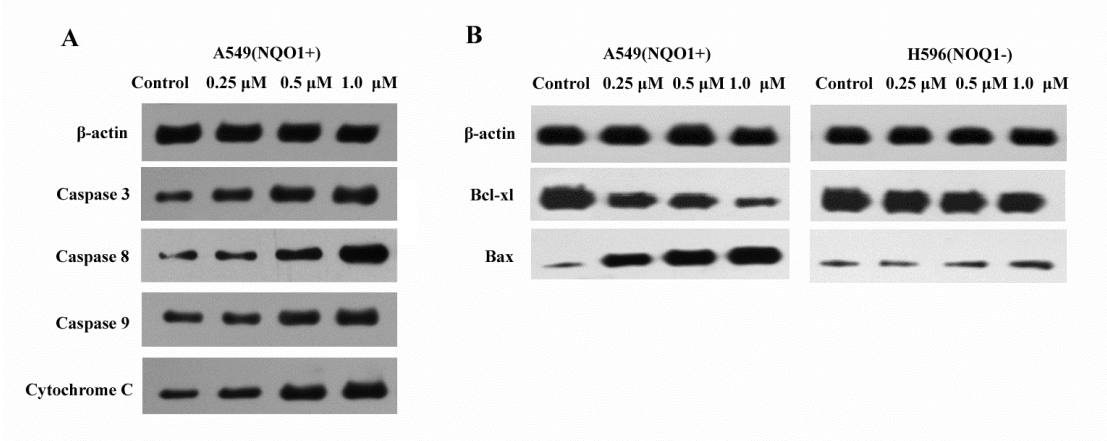

Figure 8. Effects of compound **29h** on the apoptosis related proteins. A549 and H596 cells were treated with various concentrations of **29h** (0, 0.25, 0.5, 1.0 μM) for 48h, the expressions of caspase-3, caspase-8, caspase-9, cytochrome C, Bcl-2, and Bax were determined by Western Blotting using specific antibodies, β-actin was used as internal control.

*2.8. In vivo antitumor activity of compound **29h***

To evaluate the *in vivo* antitumor activity of **29h**, liver cancer xenograft in mice was established by subcutaneous inoculation of H22 cells into the right flank of mice.

As shown in Figure 9A, compound **29h** caused a remarkable reduction in tumor growth, and reached a 64.3% reduction by the end of the observation period compared with administration of vehicle only. It is interesting to note that the effect on tumor volume reduction by **29h** was much better than that of oridonin, which caused a 50.8% of reduction at day 18. During the whole treatment period, no significant weight changes in the treated animals were observed (Figure 9D), suggesting that **29h** has minimal toxicity.

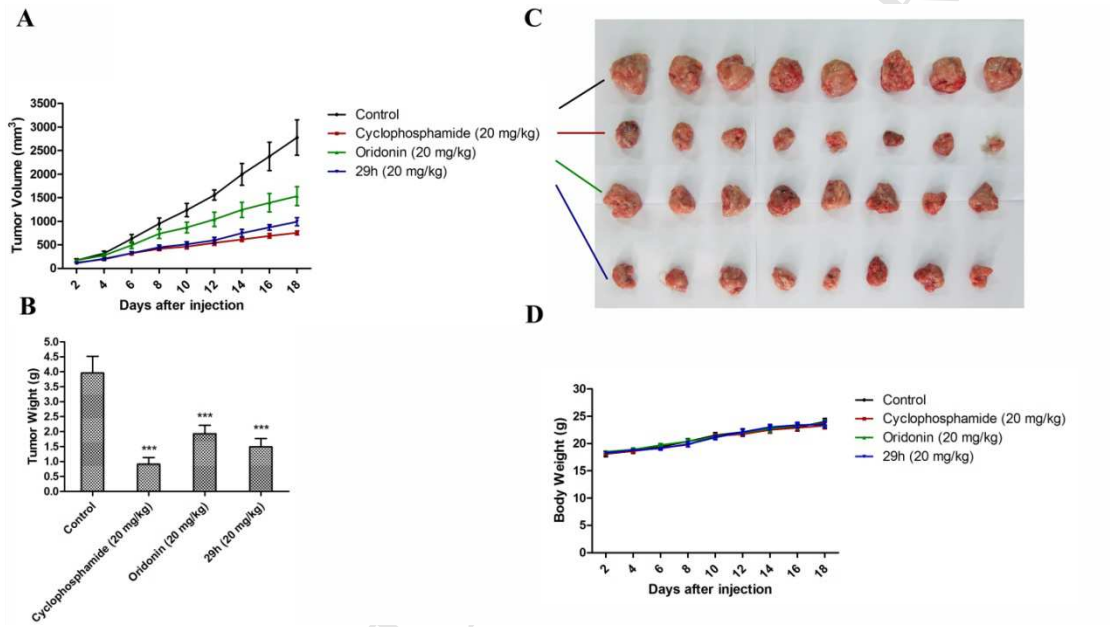

Figure 9. 29h exerted potent antitumor activity against liver cancer xenograft growth *in vivo*. (a) H22 cells were subcutaneously inoculated into the right flank of mice. The mice were randomly divided into four groups with 8 mice in each group and treated intravenously with **29h** (20 mg/kg), oridonin (20 mg/kg), cyclophosphamide (20 mg/kg), and DMSO (dissolved in sodium chloride as control) every day for 18 days and the figure showed the average measured tumor volumes; (b) **29h** treatment resulted in significantly lower tumor weight compared with control, ***P<0.001; (c) The resulting tumors were excised from the animals after treatment; (d) Body weight changes of mice during treatment.

3. Conclusion

In this study, a series of hypoxia-selective prodrugs were designed and synthesized

by functionalization of the 3-(hydroxymethyl)indolequinone with a variety of leaving groups including anticancer diterpenoids oridonin and its analogues at the (indol-3-yl)methyl position. The resulting compounds (**29a-m**) exhibited relatively high antitumor activities against NQO1-rich A549 and HT-29 cell lines, and compound **29h** has been found to be the most potent compound with IC_{50} values of 0.386 and 0.263 μM against A549 and HT-29 cells, respectively. A significant correlation between NQO1 activation and cytotoxicity was observed by using MTT assay, HPLC analysis and docking study, suggesting that indolequinone moiety contributes to the increased antiproliferative activities of targeted compounds. Moreover, the investigation of anticancer mechanism revealed that the representative compound **29h** affected cell cycle and induced NQO1 dependent apoptosis through an oxidative stress triggered mitochondria-related pathway in A549 cells. Besides, the anti-tumor activity of **29h** was verified in a liver cancer xenograft mouse model with no observable toxicity.

Overall, these NQO1-targeted oridonin prodrugs possessing indolequinone moiety represent a promising class of cytotoxic agents with potential novel therapeutic values. All properties including the cancer cell selectivity, potency, and promising *in vivo* activity of compound **29h** suggested its outstanding potential as a personalized anticancer therapy [40].

4. Experimental section

4.1. Materials

3-[4,5-dimethylthiazol-2-yl]-2,5-diphenyl-tetrazolium bromide (MTT), 5,5′,6,6′-Tetrachloro-1,1′,3,3′-tetraethyl-imidacarbocyanine iodide (JC-1), DT-diaphorase enzyme, NADH, FDA, and 2’,7’-Dichlorofluorescein diacetate (DCF-DA), were purchased from Sigma Chemical Co. (St. Louis, MO, USA). Primary antibodies against caspase-3, caspase-8, caspase-9, Bax, Bcl-xl, cytochrome C, β-actin were purchased from Beyotime (Jiangsu, China), and secondary antibodies (goat-anti-rabbit or goat-anti-mouse) were purchased from Life Technologies (Grand Island, NY, USA). All cell culture reagents including no-essential amino acids (NEAA)

and the BCA protein assay kit were purchased from Life Technologies (Grand Island, NY, USA). Institute of Cancer Research (ICR) female mice were purchased from Shanghai SLAC Laboratory Animals Co. Ltd. (China).

4.2. Cell Lines and Cell Culture

Human NSCLC cell lines A549 (NQO1+), NCI-H596 (NQO1-) and Human colon carcinoma cells HT-29 (NQO1+) were obtained from the American Type Culture Collection (ATCC, USA). Cells were grown in RPMI 1640 medium (Life Technologies, USA). The media for all cell lines were supplemented with 10% fetal bovine serum (Life Technologies, USA), 100 μg/mL streptomycin (Life Technologies, USA), and 100 U/mL penicillin (Life Technologies, USA) and maintained at 37°C in a humidified atmosphere with 5% CO_2.

4.3. Determination of In Vitro Anticancer Activity

The overall growth level of human cancer cell lines was determined by the MTT colorimetric assay. Cells were plated in 96-well plates at a density of 10000 cells/mL and incubated at 37 °C in a humidified 5 % CO_2 incubator for 24 h prior to the experiments. After medium removal, 100 μL of fresh medium containing the test compound at different concentrations was added to each well and incubated at 37 °C for 72 h, the percentage of DMSO in the medium never exceeded 0.25%. The number of living cells after 72 h of culture in the presence (or absence: control) of the various compounds is directly proportional to the intensity of the blue, which is quantitatively measured by a plate reader at 560 nm. The experiment was performed in quadruplicate and repeated 3 times.

4.4. Metabolism of 29h by DT-D

A 10 mM stock solution of **29h** was prepared in DMSO and stock solutions of 4 mM NADH and 100 μM FAD were prepared in TRIS buffer pH 7.4. The enzyme stock solution was prepared by dissolving 1.5 mg of the lyophilized human DT-Diaphorase (Sigma, ≥100 units; wherein 1 unit is 1.0 μmole cytochrome C

reduced per min/mg) in TRIS buffer pH 7.4 to make a solution of 40 mU/µL. The reaction mixture was prepared according the spreadsheet below. The reaction mixtures were stirred at 37 ^{o}C and were monitored by HPLC analysis carried out on a Prominence LC-20AT HPLC system equipped with a column (Agilent eclipse XDB C18 5µm, 4.6*250mm). The mobile phase used for elution was a linear gradient beginning with 50:50 (v/v) methanol: water at a flow rate of 1 mL/min.

Entry	Conditions	H_2O	Buffer	29h	NADH	FAD	NQO1
1	Control	80µL	40µL	600µL	40µL	40µL	0
2	With DTD	40µL	40µL	600µL	40µL	40µL	40µL
Final concentration	/	/	25 mM	0.15mM	0.2 mM	5.0 mM	2.0mU/µL

*4.5. Molecular Modelling of **29h** in NQO1*

For docking purposes, the crystallographic coordinates of the human NQO1 was obtained from Protein Data Bank, (PDB code 1H69 and resolution 1.86 Å) and the structure was edited accordingly to provide a monomer of the protein (A chain) by MOE 2014.09. Then compound **29h** was constructed using the builder molecule and was energy minimized as a MDB file. The receptor was defined as the the monomer protein and its FAD cofactor. The active site was defined as being the quinone scaffold of the original ligand in its crystal pose in the monomer of 1H69. For these experiments, the placement was set as Triangle Matcher, rescoring 1 was London dG, refinement was forcefiled, and rescoring 2 was GBVI/WSA dG. Other docking parameters were set to default. The best pose was visualized with PyMOL Molecular Graphics System version 2.7.

4.6. Hoechst 33342 Staining

Approximately 5×10^4 cells/well were planted in six-well plates, and the cells were then incubated with 0, 0.125, 0.25, 0.5 μM **29h** for 36 h. After incubation, cells were washed with PBS, fixed in 4% paraformaldehyde for 30 min and then stained with 20

μg/ml Hoechst 33342 for 15 min at room temperature in the dark. Cells were then assessed by fluorescence microscopy for morphological changes after **29h** treatment.

4.7. TUNEL assay

Terminal deoxynucleotidyl transferase-mediated Dutpnick end-labeling (TUNEL) assay was used for detection of DNA strand breaks. The detection was carried out according to the instructions of *in situ* Apoptosis Detection kit (KGA7025, Beyotime, China). Briefly, the cells were rinsed once with PBS and fixed in 3.7% buffered formaldehyde at room temperature for 10 min. The fixed cells were pre-treated with 10% H_2O_2, and end-labeling was performed with TdT labeling reaction mix at 37 °C for 1 h. Nuclei exhibiting DNA fragmentation were visualized by incubation in 3',3-diamino benzidine (Sigma) for 10 min. The cells were counter-stained with methyl green and observed under light microscopy. The nuclei of apoptotic cells were stained dark brown and TUNEL-positive cells were determined with relative percentage by randomly counting 100 cells.

4.8. JC-1 Assay to Determine MMP

The MMP was determined with the dual-emission mitochondrial dye JC-1. After treatment with 0, 0.25, 0.5, 1 μM **29h** for 36 h, A549 and H596 cells were loaded with 10 μg/mL JC-1 dye for 30 min at 37 °C and then washed for 5 min in PBS buffer. The percentage of cells with healthy or collapsed mitochondrial membrane potentials was monitored by flow cytometry analysis with an excitation wavelength of 488 nm and an emission wavelength of 530 nm an FC500 cytometer (Beckman Coulter).

4.9. Measurement of Intracellular ROS Generation

Intracellular ROS production was detected by using the peroxide-sensitive fluorescent probe DCF-DA. In brief, after treatment with 0, 0.25, 0.5, 1 μM **29h** for 36 h, A549 and H596 cells were incubated with 10 mM DCF-DA at 37 °C for 15 min. The intracellular ROS mediated oxidation of DCF-DA to the fluorescent compound 2',7'-dichlorofluorescein (DCF). Then cells were harvested and the pellets were

suspended in 1 mL PBS. Samples were analysed at an excitation wave length of 480 nm and an emission wave length of 525 nm by flow cytometry on an FC500 cytometer (Beckman Coulter).

4.10. Cell Cycle Analysis

5×10^4 cells were seeded into 6-well plates and incubated overnight. Cells were then treated with various concentrations of compound **29h** for 48 h. The cells were harvested, washed with cold PBS and then fixed with 70 % ethanol in PBS at -20 °C for 12 h. Subsequently, the cells were re-suspended in PBS containing 100 μg/ml RNase and 50 μg/ml PI and incubated at 37 °C for 30 min. Cell cycle distribution of nuclear DNA was determined by flow cytometry on an FC500 cytometer (Beckman Coulter).

4.11. Western Blot Analysis

A549 and H596 cells were incubated in the presence of **29h**, and after 48 h, were collected, centrifuged, and washed two times with ice cold PBS. The pellet was then re-suspended in lysis buffer. After the cells were lysed on ice for 20 min, lysates were centrifuged at 13000g at 4 °C for 15 min. The protein concentration in the supernatant was determined using the BCA protein assay reagents. Equal amounts of protein (20 μg) were resolved using sodium dodecyl sulfate-polyacrylamide gel electrophoresis (SDS-PAGE) (8-12 % acrylamide gels) and transferred to PVDF Hybond-P membrane. Membranes were blocked for 1 h at room temperature. Membranes were then incubated with primary antibodies against caspase-3, caspase-8, caspase-9, Bax, Bcl-xl, cytochrome C, β-actin, the membrane being gently rotated overnight at 4°C. The bound antibodies were detected using horseradish peroxidase (HRP)-conjugated second antibodies and visualized by the enhanced chemiluminescent reagent.

4.12. In vivo tumor xenograft study

Five-week-old male Institute of Cancer Research (ICR) mice were purchased from

Shanghai SLAC Laboratory Animals Co. Ltd. A total of 1×10^6 H22 cells were subcutaneously inoculated into the right flank of ICR mice according to protocols of tumor transplant research, to initiate tumor growth. After 7 d of tumor transplantation, mice in H22 group was weighted and divided into four groups of eight animals at random. The groups with oridonin and **29h** were administered intravenously 20 mg/kg in a vehicle of 10% DMF/2% poloxamer/88% saline, respectively. The positive control group was treated with cyclophosphamide (20 mg/kg) through intravenous injection. The negative control group received 0.9% normal saline through intravenous injection. All the test compounds were given through injections after 7 d of tumor transplantation. Treatment were done at a frequency of intravenous injection one dose per day for a total 18 consecutive days. Body weights and tumor volumes were measured every 2 days. After the treatments, all of the mice were killed and weighed. The following formula was used to determine tumor volumes: tumor volume = $L\times W^2/2$, where L is the length and W the width. Ratio of inhibition of tumor (%) = (1 – average tumor weight of treated group/average tumor weight of control group) $\times$ 100%. The experimental protocols were evaluated and approved by the Ethics Committee of the China Pharmaceutical University.

4.13. Synthesis of target compounds

Synthetic methods of target compounds and intermediates were reported in Supporting Information.

Acknowledgment

This work is supported by the National Natural Science Foundation (No. 81373280, 81673306), The Open Project of State Key Laboratory of Natural Medicines, China Pharmaceutical University (No. SKLNMKF201710), and China Postdoctoral Science Foundation (No. 2015M581903).

Appendix A. Supplementary data

Supplementary data related to this article can be found at

Author Contributions

[1]These authors contributed equally to this work. The manuscript was written through contributions of all authors. All authors have given approval to the final version of the manuscript.

References

[1] W.S. Shin, J.Y. Han, P. Verwilst, R. Kumar, J. H. Kim, J. S. Kim, Cancer targeted enzymatic theranostic prodrug: precise diagnosis and chemotherapy, Bioconjug. Chem. 27 (2016) 1419-1426.

[2] Y.N. Zhong, K. Goltsche, L. Cheng, F. Xie, F.H. Meng, C. Deng, Z.Y. Zhong, R. Haag, Hyaluronic acid-shelled acid-activatable paclitaxel prodrug micelles effectively target and treat CD44-overexpressing human breast tumor xenografts in vivo, Biomaterials. 84 (2016) 250-261.

[3] Y. Kim, A.E. Maciag, Z. Cao, J.R. Deschamps, J.E. Saavedra, L.K. Keefer, R.J. Holland, PABA/NO lead optimization: improved targeting of cytotoxicity to glutathione S-transferase P1-overexpressing cancer cells, Bioorg. Med. Chem. 23 (2015) 4980-4988.

[4] V. Liapis, I. Zinonos, A. Labrinidis, H. Shelley, V. Ponomarev, V. Panagopoulos, A. Zysk, M. DeNichilo, W. Ingman, G.J. Atkins, D.M. Findlay, A.C.W. Zannettino, A. Evdokiou, Anticancer efficacy of the hypoxia-activated prodrug evofosfamide (TH-302) in osteolytic breast cancer murine models, Cancer Medicine 5 (2016) 534-545.

[5] Y. Singh, M. Palombo, P.J. Sinko, Recent trends in targeted anticancer prodrug and conjugate design, Curr. Med. Chem. 15 (2008) 1802-1826.

[6] M. Erkan, M. Kurtoglu, J. Kleeff, The role of hypoxia in pancreatic cancer: a potential therapeutic target? Expert. Rev. Gastroent. 10 (2016) 301-316.

[7] P. Vaupel, A. Mayer, Hypoxia in cancer: significance and impact on clinical outcome, Cancer Metast. Rev. 26 (2007) 225-239.

[8] R.M. Phillips, Targeting the hypoxic fraction of tumours using hypoxia-activated prodrugs, Cancer Chemother. Pharmacol. 77 (2016) 441-457.

[9] J.L. Wang, C.P. Guise, G.U. Dachs, Y. Phung, H.L. Hsu, N.K. Lambie, A.V. Patterson, W.R. Wilson, Identification of one-electron reductases that activate both the hypoxia prodrug SN30000 and diagnostic probe EF5, Biochem. Pharmacol. 91 (2014) 436-446.

[10] E.T. Oh, H.J. Park, Implications of NQO1 in cancer therapy, BMB Rep. 48 (2015) 609-617.

[11] Q.A. Best, A.E. Johnson, B. Prasai, A. Rouillere, R.L. McCarley, Environmentally robust rhodamine reporters for probe-based cellular detection of the cancer-linked oxidoreductase hNQO1, ACS Chem. Biol. 11 (2016) 231-240.

[12] Y. Yang, Y. Zhang, Q.Y. Wu, X.L. Cui, Z.H. Lin, S.P. Liu, L.Y. Chen, Clinical implications of high NQO1 expression in breast cancers, J. Exp. Clin. Cancer Res. 33:14 (2014) 1-9.

[13] E.I. Parkinson, P.J. Hergenrother, Deoxynyboquinones as NQO1-activated cancer therapeutics, Acc. Chem. Res. 48 (2015) 2715-2723.

[14] H.R. Nasiri, M.G. Madej, R. Panisch, M. Lafontaine, J.W. Bats, C.R. Lancaster, H. Schwalbe, Design, synthesis, and biological testing of novel naphthoquinones as substrate-based inhibitors of the quinol/fumarate reductase from Wolinella succinogenes, J. Med. Chem. 56 (2013) 9530-9541.

[15] K.W. Wellington, Understanding cancer and the anticancer activities of naphthoquinones -a review. RSC Adv. 5 (2015) 20309-20338.

[16] M. Jaffar, N. Abou-Zeid, L. Bai, I. Mrema, I. Robinson, R. Tanner, I. J. Stratford, Quinone bioreductive prodrugs as delivery agents, Curr. Drug. Deliv. 1 (2004) 345-350.

[17] D. Ross, D. Siegel, H.D. Beall, A.S. Prakash, R.T. Mulcahy, N.W. Gibson, DT-diaphorase in activation and detoxification of quinones. Bioreductive activation of mitomycin C, Cancer Metast. Rev. 12 (1993) 83-101.

[18] R.M. Phillips, H.R. Hendriks, G.J. Peters, EORTC-Pharmacology and Molecular Mechansims Group. EO9 (Apaziquone): from the clinic to the laboratory and back again, Brit. J. Pharmacol. 168 (2013) 11-18.

[19] V. Yutkin, J. Chin, Apaziquone as an intravesical therapeutic agent for urothelial non-muscle-invasive bladder cancer, Expert Opin. Investig. Drugs 21 (2012) 251-260.

[20] C.P. Guise, A.M. Mowday, A. Ashoorzadeh, R. Yuan, W.H. Lin, D.H. Wu, J.B. Smaill, A.V. Patterson, K. Ding, Bioreductive prodrugs as cancer therapeutics: targeting tumor hypoxia, Chin. J. Cancer. 33 (2014) 80-86.

[21] J.J. Newsome, M. Hassani, E. Swann, J.M. Bibby, H.D. Beall, C.J. Moody, Benzofuran-, benzothiophene-, indazole- and benzisoxazole-quinones: Excellent substrates for NAD(P)H: quinone oxidoreductase 1, Bioorg. Med. Chem. 21 (2013) 2999-3009.

[22] J. Sasaki, K. Sano, M. Hagimori, M. Yoshikawa, M. Maeda, T. Mukai, Synthesis and in vitro evaluation of radioiodinated indolequinones targeting NAD(P)H: quinone oxidoreductase 1 for internal radiation therapy, Bioorg. Med. Chem. 22 (2014) 6039-6046.

[23] M.A. Naylor, E. Swann, S.A. Everett, M. Jaffar, J. Nolan, N. Robertson, S.D. Lockyer, K.B. Patel, M.F. Dennis, M.R.L. Stratford, P. Wardman, G.E. Adams, C.J. Moody, I.J. Stratford, Indolequinone antitumor agents: reductive activation and elimination from (5-Methoxy-1-methyl-4,7-dioxoindol-3-yl)methyl derivatives and hypoxia-selective cytotoxicity in vitro, J. Med. Chem. 41 (1998) 2720-2731.

[24] B.H. Huang, A. Desai, S.Z. Tang, T.P. Thomas, J.R Baker Jr, The synthesis of a c(RGDyK) targeted SN38 prodrug with an indolequinone structure for bioreductive drug release, Org. Lett. 12 (2010) 1384-1387.

[25] K. Tanabe, H. Harada, M. Narazaki, K. Tanaka, K. Inafuku, H. Komatsu, T. Ito, H. Yamada, Y. Chujo, T. Matsuda, Monitoring of biological one-electron reduction by ^{19}F NMR using hypoxia selective activation of an ^{19}F-labeled indolequinone derivative, J. Am. Chem. Soc. 131 (2009) 15982-15983.

[26] K. Sharma, A. Iyer, K. Sengupta, H. Chakrapani, INDQ/NO, a bioreductively activated nitric oxide prodrug, Org. Lett. 15 (2013) 2636-2639.

[27] M. Hernick, C. Flader, R. F. Borch, Design, synthesis, and biological evaluation of indolequinone phosphoramidate prodrugs targeted to DT-diaphorase, J. Med. Chem. 45 (2002) 3540-3548.

[28] B.H. Huang, S.Z. Tang, A. Desai, X.M. Cheng, A. Kotlyar, A. Van Der Spek, T.P. Thomas, J.R. Baker Jr, Human plasma-mediated hypoxic activation of indolequinone-based naloxone pro-drugs, Bioorg. Med. Chem. Lett. 19 (2009) 5016-5020.

[29] E. Fujita, Y. Nagao, K. Kaneko, S. Nakazawa, H. Kuroda, The antitumor and antibacterial activity of the Isodon diterpenoids, Chem. Pharm. Bull. 24 (1976) 2118-2127.

[30] Y. Ding, C.Y. Ding, N. Ye, Z.Q. Liu, E.A. Wold, H.Y. Chen, C. Wild, Q. Shen, J. Zhou, Discovery and development of natural product oridonin-inspired anticancer agents, Eur. J. Med. Chem. 122 (2016) 102-117.

[31] T. Ikezoe, S.S. Chen. X.J. Tong, D. Heber, H. Taguchi, H.P. Koeffler, Oridonin induces growth inhibition and apoptosis of a variety of human cancer cells**,** Int. J. Oncol. 23 (2003) 1187-1193.

[32] S.T. Xu, H. Yao, S.S. Luo, Y.K. Zhang, D.H. Yang, D.H. Li, G.Y. Wang, M. Hu, Y.Y. Qiu, X.M. Wu, H.Q. Yao, W.J. Xie, Z.S. Chen, J.Y. Xu, A novel potent anticancer compound optimized from a natural oridonin scaffold induces apoptosis and cell cycle arrest through the mitochondrial pathway, J. Med. Chem. 60 (2017) 1449-1458.

[33] S.T. Xu, S.S. Luo, H. Yao, H. Cai, X.M. Miao, F. Wu, D.H. Yang, X.M. Wu, W.J. Xie, H.Q. Yao, Z.S. Chen, J.Y. Xu, Probing the anticancer action of oridonin with fluorescent analogues: Visualizing subcellular localization to mitochondria, J. Med. Chem. 59 (2016) 5022-5034.

[34] S.T. Xu, L.L. Pei, C.Q. Wang, Y.K. Zhang, D.H. Li, H.Q. Yao, X.M. Wu, Z.S. Chen, Y.J. Sun, J.Y. Xu, Novel hybrids of natural oridonin-bearing nitrogen

mustards as potential anticancer drug candidates, ACS Med. Chem. Lett. 5 (2014) 797-802.

[35] J.Y. Xu, J.Y. Yang, Q. Ran, L. Wang, J. Liu, Z.X. Wang, X.M. Wu, W.Y. Hua, S.T. Yuan, L.Y. Zhang, M.Q. Shen, Y.F. Ding, Synthesis and biological evaluation of novel 1-O- and 14-O-derivatives of oridonin as potential anticancer drug candidates, Bioorg. Med. Chem. Lett. 18 (2008) 4741-4744.

[36] A. Schäfer, E.S. Burstein, R. Olsson, Bexarotene prodrugs: Targeting through cleavage by NQO1 (DT-diaphorase), Bioorg. Med. Chem. Lett. 24 (2014) 1944-1947.

[37] L.Y. Yang, Q.N. Liang, K. Shen, L. Ma, N. An, W.P. Deng, Z.W. Fei, J.W. Liu, A novel class I histone deacetylase inhibitor, I-7ab, induces apoptosis and arrests cell cycle progression in human colorectal cancer cells, Biomed. Pharmacother. 71 (2015) 70-78.

[38] P.Y. Yang, D.N. Hu, Y.H. Kao, I.C. Lin, C.Y. Chou, Y.C. Wu, Norcantharidin induces apoptosis in human prostate cancer cells through both instrinsic and extrinsic pathways, Pharmacol. Rep. 68 (2016) 874-880.

[39] E.J. Hennessy, Selective inhibitors of Bcl-2 and Bcl-x(L): Balancing antitumor activity with on-target toxicity, Bioorg. Med. Chem. Lett. 26 (2016) 2105-2114.

[40] E.I. Parkinson, J.S. Bair, M. Cismesia, P.J. Hergenrother, Efficient NQO1 substrates are potent and selective anticancer agents, ACS Chem. Biol. 8 (2013) 2173-2183.

Lists of Captions:

Figure 1. Chemical structures of antitumor quinones.

Figure 2. Schematic illustration for activation of NQO1-targeted prodrugs upon hypoxic irradiation.

Figure 3. NQO1 contributes to the cytotoxicity of these newly designed indolequinone prodrugs. (A) Compounds induced cytotoxicity is NQO1 dependent. A549 cells were pretreated with 10 mM DIC for 30 min, then incubated with indicated compounds, DIC (dicoumarin), NQO1 inhibitor; (B) Comparison of anticancer activity of compound **29h** with that of equimolar mixture of **13** and **27**. MTT methods, cells were incubated with indicated compounds for 72h, (means ± SD, n=3).

Figure 4. These newly synthesized prodrugs are good substrates of NQO1. (A) Decomposition profiles of **29h** in the presence and absence of NQO1 were determined by HPLC analysis. (B) Docked conformation of compound **29h** into active site of NQO1. The interaction mode was obtained through molecular docking (PDB id: 1h29) and depicted using PyMOL. FAD is expressed in magenta and **29h** is represented as stick model, nitrogen atoms are colored in blue, oxygen atoms are colored in red, and carbon atoms are colored in cyan. Hydrogen bonds are represented by dashed yellow lines along with their distances.

Figure 5. Evidence shows that compound **29h** induces apoptosis. (A) Cell morphological alterations and nuclear changes associated with A549 and H596 cells after **29h** treatment were assessed by staining with Hoechst 33342 and visualized by fluorescence microscopy. *** $p < 0.001$ compared between A549 and H596 groups. (B) TUNEL assay was used to identify apoptosis. Histograms display the percentage

of apoptotic cells. Data were represented as mean ± SD of three independent experiments. *** $p < 0.001$ *vs* control group.

Figure 6. The depolarization of mitochondrial membrane potential and accumulation of ROS production induced by **29h** are required for cell apoptosis. (A) Effect of **29h** on ROS generation. The generation of ROS was measured by using the ROS-detecting fluorescent dye DCF-DA in combination with FACScan flow cytometry. The corresponding histograms of FACScan flow cytometry is shown; (B) Effect of compound **29h** on the mitochondrial membrane potentials of A549 cells. A549 cells were incubated with the indicated concentrations of compound **29h** for 48 h, cells were then collected and stained with JC-1, followed by flow cytometric analysis.

Figure 7. Compound **29h** induces G2/M phase arrest in the A549 cells. A549 cells were treated with DMSO and varying concentrations of **29h** (0.125, 0.25, 0.5 μM) for 48 h, cells were harvested and stained with PI, then analyzed by flow cytometry. The percentage of cells at different phases of cell cycle was determined by ModFit 4.1, histograms display the percentage of cell cycle distribution.

Figure 8. Effects of compound **29h** on the apoptosis related proteins. A549 and H596 cells were treated with various concentrations of **29h** (0, 0.25, 0.5, 1.0 μM) for 48h, the expressions of caspase-3, caspase-8, caspase-9, cytochrome C, Bcl-2, and Bax were determined by Western Blotting using specific antibodies, β-actin was used as internal control.

Figure 9. 29h exerted potent antitumor activity against liver cancer xenograft growth *in vivo*. (a) H22 cells were subcutaneously inoculated into the right flank of mice. The mice were randomly divided into four groups with 8 mice in each group and treated intravenously with **29h** (20 mg/kg), oridonin (20 mg/kg), cyclophosphamide (20

mg/kg), and DMSO (dissolved in sodium chloride as control) every day for 18 days and the figure showed the average measured tumor volumes; (b) **29h** treatment resulted in significantly lower tumor weight compared with control, ***P<0.001; (c) The resulting tumors were excised from the animals after treatment; (d) Body weight changes of mice during treatment.

Scheme 1. Synthesis of oridonin analogues **11**-**20**[a]

Scheme 2. Synthesis of NQO1-targeted prodrug candidates **29a-n**[a]

Table 1. IC_{50} values (μM) of final and reference compounds on inhibiting proliferation of human cancer and normal cells[a]

Highlights

1. NQO1-targeted oridonin prodrugs possessing indolequinone moiety were prepared.

2. They showed relatively higher antineoplastic activities against NQO1-rich cancer cells.

3. The most potent compond **29h** is a good substrate of NQO1.

4. The anti-tumor activity of **29h** was verified in a liver cancer xenograft mouse model.